The Band Spectrum of OH^+

F. W. LOOMIS AND W. H. BRANDT, *University of Illinois*

(Received October 17, 1935)

Two bands at 3332 and 3565A discovered by Rodebush and Wahl in the electrodeless discharge in pure water vapor, and two new bands at 3695 and 3893A, are shown to be, respectively, the (1,0), (0,0), (1,1) and (0,1) bands of OH^+. Rotational analysis establishes that they correspond to a $^3\Pi \rightarrow {}^3\Sigma^-$ transition in which the $^3\Pi$ state is inverted, with coupling intermediate between cases *a* and *b*. The nine strong branches to be expected in this type of transition are found, and also enough satellite branches (nine in the 0,0 band) to determine the multiplet intervals in both states. The Λ type doubling is large and there are exceptionally large perturbations in the $3b$, $2a$ and $1b$ levels of the $v'=1$ state, with maxima at approximately $K'=18.5$, 14.5 and 10.5, respectively. These perturbations are attributed to another $^3\Sigma^-$ state. The $^3\Sigma^-$ state concerned in the transition and the perturbing state are molecular levels which dissociate into the ground states of O and H^+ and O^+ and H, respectively, but one cannot tell which is which. The $^3\Pi$ state probably dissociates into the ground states of O and H^+.

I. INTRODUCTION

IN the course of an investigation of certain problems in the chemical behavior of the OH radical, Rodebush and Wahl[1] discovered two new bands with heads at 3564 and 3328A, degraded to the red. Their source was the electrodeless discharge in very pure water vapor, and the bands have the coarse structure characteristic of diatomic hydrides, so that it seemed very likely that the carrier of these bands is some form of OH, probably the ion OH^+. However, the spectrum of OH has been the subject of numerous investigations and it is a little surprising that, if these rather strong bands are due to its ion, they should not have been discovered before. Moreover, it is to be expected that the bands of OH^+ will be analogous to those of the isoelectronic molecule NH. But the latter are known and are, superficially at least, very different, since they are of the headless type, while the new ones are sharply degraded to the red. It was clear that the question could best be settled by a detailed investigation of the rotational structure of the new bands.

A preliminary investigation[2] disclosed the fact that the bands have an extraordinarily complex structure and that the resolving power of a large grating would be necessary for their analysis. This was undertaken, using some modifications of the source described by Rodebush and Wahl, the principal change being the use of a D-shaped discharge tube with the exciting coil wound around the curved part and the spectrum viewed along the straight part. A rather critical adjustment of the pressure in the discharge tube was necessary. If the pressure was too low, the conditions were apparently too spark-like, the discharge appeared purple and spectrograms showed that most of the energy went into the oxygen spark spectrum. If the pressure was too high, the discharge either did not occur or, if it did, was bluish white and the new bands were not intense. The actual pressure used was not measured, but was probably a few hundredths of a millimeter. The discharge was red and the Balmer series prominent. The "water" bands appeared with great intensity, nearly all of the lines which have been reported in the literature and which occur in the region measured being observed. An important advantage of this electrodeless discharge is the suppression of the hydrogen continuum, which ordinarily practically obscures the region where the new bands occur. This is due to the fact that, in the complete absence of a metal catalyst, the hydrogen molecules are not formed.

Satisfactory photographs were obtained in the first order of a 6-inch 30,000-line/inch, 21-foot concave grating with a dispersion of 1.25A/mm with 20 hours exposure. To increase the intensity a slit width of 0.04 mm was used which is too great to give the full resolving power of the grating. The photographs disclosed a new band with its head at 3983A, which is the (0,1) band of the system of which those discovered by Rodebush and Wahl are the (1,0) and (0,0)

[1] Rodebush and Wahl, J. Chem. Phys. **1**, 696 (1933).
[2] With H. M. Pepiot.

TABLE A. *Wave-lengths of OH^+ band heads.*

$v' \backslash v''$	0	1
0	3565	3893
1	3332	3695

bands. The analysis showed that the wave-lengths of the heads of the bands, as reported by Rodebush and Wahl, are slightly too low, because of a fortuitous accumulation of other lines in the neighborhood. The analysis also disclosed many of the stronger lines of the (1,1) band, especially of the Q branches, intermingled with those of the (0,0) band. The correct wave-lengths of the heads of these four bands (the R_3 branches) are given in Table A, that for the (1,1) band having been computed from the four band combination relations for the R_3 branches.

II. ANALYSIS

1. Strong branches

Observation of the bands reveals that the stronger lines occur in series of groups of three. This indicates that the states involved are triplets. By analogy[3, 4] with NH and PH one would expect to find bands in OH^+ belonging to a $^3\Pi \rightarrow {}^3\Sigma$ transition with the $^3\Pi$ state approaching case a for low K values and case b for high K values. The analysis shows that this is the case and that the $^3\Pi$ state is inverted. The possible transitions from a $^3\Pi$ to a $^3\Sigma$ state are shown in Fig. 1. The full lines represent strong transitions, the dashed lines weaker ("satellite") transitions and the dotted lines very weak transitions. There are nine strong branches, three P, three Q and three R. Most of these branches were found by inspection and extended by second differences. A few of the branches could not be accurately assigned before enough was known about the quantum numbers to use combination differences.

The three lines in each of the distinct triplets into which the strong lines arrange themselves at some distance from the origin are known to have the same value of K, since case b is here closely approached. The clue to the *relative* numbering of the lines lies in a consideration of the internal triplet spacings in the several

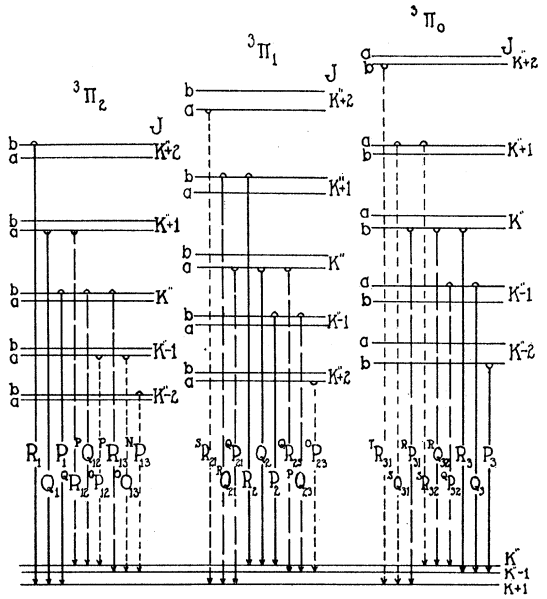

FIG. 1. Schematic representation of possible transitions between $a\ ^3\Pi$ and $a\ ^3\Sigma$ state. Full lines are strong transitions, dashed lines are weaker transitions and dotted lines are very weak transitions. The character of Λ type doubling is indicated qualitatively for K values <13.

branches. That is, the quantum numbers K' and K'' can be assigned, except for a single additive integer, common to all branches, from a study of the magnitudes of the intervals $Q_3(M)-Q_2(M)$, $Q_2(M)-Q_1(M)$, etc. Neglecting the presumably small variation of the internal spacing of the triplet levels in the $^3\Sigma$ state with K'', and also the variation in the internal triplet spacing with Λ type doubling, the same value of K' was assigned to triplets in each of the three sets of branches which have the same internal spacings; and similarly, neglecting the variation of the internal $^3\Sigma$ spacing with v'', the same value of K' was assigned to corresponding triplets in the (0,0) and (0,1) bands. The P, Q and R branches could then be distinguished by the criterion $\nu_R(K) > \nu_Q(K) > \nu_P(K)$. Subsequently the assignments were fully checked by the combination relations which are wholly independent of the above approximations. The assignment of relative K values to the (1,0) band was similar though less certain, but was eventually checked by combinations.

Absolute K values were determined by plotting $\Delta_2 F_2''(M)$ and extrapolating to zero at $K''=-\frac{1}{2}$. The set of components, F_2, was used since $\Delta_2 F_2''$

[3] Batsch, Ann. d. Physik **410**, 81 (1933).
[4] Pearse, Proc. Roy. Soc. **A129**, 328 (1930).

involves no term in $f_i(K, J-K)$. See Eqs. (2)–(5).

2. Perturbations

There are three perturbations in the $^3\Pi$ level ($v=1$). These appear only in the (1, 0) band, since the branches of the (1,1) band are too weak for observation in the perturbed regions. These perturbations occur as given in Table B.

TABLE B.

LEVEL PERTURBED	K' OF MAXIMUM PERTURBATION	BRANCHES INVOLVED
F_{3b}	18.5	P_3, R_3
F_{2a}	14.5	Q_2
F_{1b}	10.5	P_1, R_1

The perturbation in the F_{2a} level involves only the Q_2 branch and there are no exact combinations to check the assignment. However, since the Q branches are quite intense and since the Q_2 branch is the middle branch, this perturbation shows up strikingly on the figure and the assignments are evident by observation. Fig. 5 shows this perturbation. In the case of the P_3, R_3 and P_1, R_1 branches the intensities are not sufficiently greater than those of neighboring lines to establish the assignment beyond doubt. However, all attempts to assign smooth branches in these regions were unsuccessful and Tables II and V show that the intensities as assigned are smooth and that the Δ_2F'' values agree to within experimental error with those of the (0,0) band. These two factors make the assignment seem quite valid.

Accompanying a perturbation there should be faint lines due to transitions to the perturbing state. These lines may well be present but cannot be assigned because of the great number of faint lines in those regions.

3. "Satellite" and very weak branches

The assignment of "satellite" branches will be discussed in connection with multiplet splitting in the $^3\Sigma$ state. When all branches corresponding to full and dashed lines in Fig. 1 are known, the fainter branches can be accurately predicted by combinations.[5] Of these only the $^SR_{32}$ branch of the (0,0) band was observed. No "satellite" or very faint branches were observed in the (0,1) band since this band is comparatively weak.

From a consideration of the low lying states of O and O^+ which might, according to the rules of Wigner and Witmer,[6] yield the $^3\Sigma$ and $^3\Pi$ states involved in the spectral transition, and which might, according to Kronig's[7] rules, perturb the $^3\Pi$ state, one finds that only four states may be concerned: namely, a $^3\Sigma^-$ state which dissociates into $^4S^\circ$ of O^+ and 1^2S of H, a $^3\Pi$ state which dissociates into $^2D^\circ$ of O^+ and 1^2S of H, and a $^3\Sigma^-$ and a $^3\Pi$ state which dissociates into ^3P of O and H^+. One concludes that the $^3\Sigma$ state observed is one of these $^3\Sigma^-$ states, that the $^3\Pi$ state observed is one of these $^3\Pi$ states and that the perturbing state is either the other $^3\Sigma^-$ or the other $^3\Pi$ state. It is very likely that the perturbing state is $^3\Sigma^-$ since it could produce just the perturbations observed, whereas a $^3\Pi$ state would be likely to produce more. If the heats of dissociation which can be calculated from the values of ω and ωx given below can be relied upon even very roughly, within say 3 volts out of 4 and 1, respectively, one may conclude that the $^3\Pi$ state which dissociates into O^+ $^2D^\circ$ cannot be concerned in the transition observed. One may then conclude that one of the two $^3\Sigma^-$ states which dissociate into normal O and H^+ and normal O^+ and H, respectively, is the ground state of the OH^+ molecule, the other being the perturbing state; also that the observed $^3\Pi$ state is the one which dissociates into ^3P of O and H^+.

III. DATA

The frequencies of lines which have been assigned to branches are recorded in Tables I–III. The intensities are visual estimates made while measuring plates; d after the intensity indicates that the line is diffuse. A number in parenthesis indicates that the line has been assigned that number of times. Since the "water" bands overlap the (1,0) and the (0,0) bands, not all of these occur twice in the tables. Except in the region of the (0,0) band, there are numerous

[5] For the notation used here and for an exhaustive list of combination relations in $^3\Pi - {}^3\Sigma$ bands see Naudé, Proc. Roy. Soc. **A136**, 114 (1930).

[6] Wigner and Witmer, Zeits. f. Physik **51**, 859 (1928).

[7] Kronig, Zeits. f. Physik **50**, 347 (1928).

TABLE I. *Branches of (0,0) band.*

K	INT.	ν (vac)	INT.	ν (vac)	INT.	ν (vac)
		R_3		R_2		R_1
1	1	28040.55				
2	2	044.96	1	28009.23	1	27954.13
3	2	044.41	5	015.28 (2)	3	968.45
4	1	039.73	5	014.72 (2)	5	975.66 (2)
5	4	030.18 (2)	2	008.20 (2)	5	975.66 (2)
6	5	015.28 (2)	2	27995.89	4	967.61 (2)
7	2	27994.49	2	977.17	4	953.05 (2)
8	4	967.61 (2)	4	951.96	5	930.80 (2)
9	5	933.89 (4)	4	920.05 (2)	3	901.33
10	3	893.85	5	881.19 (3)	2	864.68
11	3	846.65	4	835.18 (3)	4	820.60
12	5	792.76 (2)	3	782.09 (2)	2d	769.15
13	2	731.09	3	721.81 (3)	3	710.08
14	2	662.24	4	653.64	2	643.34
15	4	585.69 (2)	10	578.15 (2)	2	568.66
16	1	501.32	2	494.23	2	485.96
17	2	408.91	2	402.40 (2)	2	395.20
18	2	308.36	2	302.55	2	296.05
19	2d	199.07	1	193.88	2	188.28
20	2	081.45	2	076.66	2	071.75
21	2	26954.72	2	26950.43	2d	946.19
22	1	818.90	3	815.08 (2)	2	811.47
23	1	673.66	1	670.18	2d	667.27
24	1d	518.52	0d	515.68	1d	512.81
25	1	353.65	1	350.83 (2)	1	349.28
26	1d	178.59	0	175.03	1d	176.70
27	0d	993.11				
28	1	796.44				
		Q_3		Q_2		Q_1
1	2	28008.20 (2)				
2	1	27982.69	5	27930.80 (2)	2	27864.68 (2)
3	4	953.05 (2)	2	909.00	3	855.02
4	4	920.05 (2)	5	881.19 (3)	4	837.66 (2)
5	3	882.45 (2)	3	848.36	5	812.35 (2)
6	4	840.22	5	809.54 (2)	5	779.65 (2)
7	5	792.76 (2)	3	764.94	20	739.78 (2)
8	20	739.78 (2)	5	714.39	7	692.86
9	7	680.96 (2)	6	657.42 (3)	6	638.99
10	5	616.24	4	594.36 (2)	10	578.15 (2)
11	7	545.21	6	524.69	3	510.79 (2)
12	6	467.70	6	448.47	7	436.28
13	5	383.66	7	365.59	6	354.85
14	6	292.92	6	275.87	6	266.39
15	5	195.25	7	179.12	8	170.84
16	5	090.64	6	075.33	6	068.03
17	6	26978.80 (2)	6	26964.23	6	26957.80
18	5	859.71	5	845.82	5	840.15
19	8	732.94	8	719.77	8	714.87
20	4	598.73	5	586.17	5	581.77
21	4	456.55	4	444.51	4	440.78
22	2	305.72	3	294.79	3	291.54
23	8	147.53	8	136.68	5	133.96
24	3	25980.85	3	25970.38	2	25968.07
25	4	805.23	2	795.01	2	793.17
26	1	620.32	1	610.75	1	609.38
27	0	426.31	1	417.17	1	416.32
28	00	222.89	2	213.90		
29	2	009.93 (2)	2	001.14 (2)		
30	0	24786.04				
		P_3		P_2		P_1
1						
2	5	27933.89 (4)	1	27884.97 (2)	1	27798.26
3	1d	876.56	4	835.18 (3)	1	766.07 (2)
4	1	815.19	5	779.65 (2)	1	724.44
5	1	749.84	1	720.53	1	674.79
6	7	680.96 (2)	1	655.93 (2)	1	617.52
7	2	607.22	4	585.69 (2)	3	553.25
8	2	528.87	1	509.80	3	482.03

K	INT.	ν (vac)	INT.	ν (vac)	INT.	ν (vac)
		P_3		P_2		P_1
9	3	445.29	3	428.35	2	404.33
10	4	356.27	5	341.08	5	320.12
11	4	261.65	3	248.03	6	229.60
12	4	161.29	4	148.94	5	132.65
13	5	054.98	5	043.81	6	029.43
14	6	26942.65	6	26932.59	6	26919.81
15	2	824.26	3	815.08 (2)	4	803.75
16	4	699.69	4	691.34	4	681.23
17	4	568.76	4	561.21	4	552.21
18	4	431.35	4	424.46	4	416.58
19	3	287.39 (2)	3	281.17	3	274.23 (2)
20	8	136.68 (2)	3	131.09	3	124.95
21	3	25979.29	3	25974.19	2	25968.71
22	2	814.56	2	810.04	4	805.23 (3)
23	1	642.71	1	638.67	1	634.73
24	0	463.64	1	459.98	1	456.56
25	1	276.74	1	273.69	1	270.67
26	0	082.09	0d	078.84 (2)	0	076.90 (2)
27	2	24877.65 (2)			1	24875.14
28					00	666.35
29					00	451.21
30					1	228.05
31					00	995.68
		$^RQ_{21}$		$^RQ_{32}$		$^QP_{32}$
1	1	28000.23				
2	2d	011.52 (2)	2d	28042.38 (2)	1	27980.42 (2)
3	2	017.29 (2)	2d	042.38 (2)	1d	949.86
4	2	017.29 (2)	1	037.82	1	918.29
5	2d	011.52 (2)	1	028.64	5	881.19 (3)
6	1	27999.06	5	014.72 (2)	1	838.89 (2)
7	1	980.42 (2)	1	993.20	1d	789.73 (2)
8	1	955.32	1	966.44		
9	1	923.45				
10	1	884.97 (2)				
11	1	838.89 (2)				
12	1d	786.41 (2)				
		$^QP_{21}$		$^QR_{23}$		$^QR_{12}$
2	5	27933.89 (4)	5	27933.89 (4)	2	27861.56
3	1	911.28 (2)	1	911.28 (2)	1d	852.29 (2)
4	1	27883.86	3	882.45 (2)	4	835.18 (3)
5	1	851.11	2	849.91 (2)	5	809.54 (2)
6	5	812.35 (2)	1	811.01	1	776.57
7			1	766.07	1d	736.52
8	1	717.67			1	689.40
9	1d	661.06	1d	659.19	1	635.42
10	1	598.15			0	574.62
11	2	528.87 (2)				
12	1	452.29 (3)				
		$^PQ_{23}$		$^PQ_{12}$		$^SR_{32}$
1					1	28112.64
2			1	27795.93	0	147.34
3	4	27837.66 (2)	1	763.38	1	175.28
4	3	782.09 (2)	3	721.81 (3)	1d	197.14
5	3	721.81 (3)	1d	671.88	2d	212.41 (2)
6	6	657.42 (3)	1	614.49	1	220.83
7	1	586.87	1	549.94		
8	3	510.79 (2)	1	478.65		
9	00	429.34	1	400.75		
10			1	316.52		
11			1	225.74		
12			0	128.67		
13			1	025.27		
14			0	26915.56		
15			00	799.48		

lines which have not been assigned, but none of them are stronger than intensity "2".

Combination differences are given in Tables IV–VII inclusive.

Corresponding values of $\Delta_2 F_i''$ agree to within experimental error for the (0,0) and (1,0) bands and corresponding values of $\Delta_1 F_{iab}'$, $\Delta_1 F_{iba}'$ and $\Delta_2 F_{ib}'$ agree to within experimental error for the (0,0) and (0,1) bands. Table IV(a) shows observed frequencies of Q branches of the (1,1) band. Table IV(b) shows the values of these frequencies calculated by 4 band combinations.

TABLE II. *Branches of (1,0) band.*

K	INT.	ν (vac)	INT.	ν (vac)	INT.	ν (vac)
		R_3		R_2		R_1
1						
2					3	29917.79
3	1	30004.72			2	926.38
4	1	29993.12	1	29964.26	2	925.04
5	4	973.20	3	947.77	3	914.67
6	3	946.23	2	923.68	5	895.14
7	2	911.63	5	891.52 (2)	5	866.94
8	5	869.27	3	850.97	4	829.91
9	3	818.78	6	802.05 (2)	5	785.03
10	4	759.90	6	744.73	6	724.43
11	10	692.58	8	678.62	5	662.44 (2)
12	6	616.70	6	603.83	6	589.78
13	6	532.11	6	519.99	8	507.49
14	5	438.54 (2)	5	427.08	3	415.96
15	5	335.89	4	324.81	5	314.98 (2)
16	6	224.73	3	213.23	2	204.60
17	3	107.47	10	091.96 (2)	10d	084.60 (2)
18	3	28958.06	3	28960.95 (2)	3	28954.17
19	1	822.58	7	819.84 (2)	2	814.04
20	2	672.25	3	668.37 (2)	4d	663.85
21	1	510.42	1	506.79	2	503.09 (2)
22	1	337.69	1	334.59 (2)	1	334.59 (2)
23	2	154.20 (2)	1	151.31		
24	1	27959.32	1	27956.92		
25			00	751.35		
26			0	534.23		

K	INT.	ν (vac)	INT.	ν (vac)	INT	ν (vac)
		Q_3		Q_2		Q_1
1			2	29926.38	3	29841.16 (2)
2	1	29955.22	2	904.29	1	835.07
3	1	920.02	5	875.21	3	819.37
4	4	879.42	3	841.16	6	795.25
5	5	833.41	4	799.94	5	761.41
6	5	780.59	6	751.10	6	718.49
7	6	721.33	9	694.78	6	666.78
8	6	654.72	7	630.20	10	606.30 (2)
9	10	580.78	7	558.87	8	537.37
10	10	498.95	10	479.18	10	459.84
11	10	409.40	10	391.38	10	373.87
12	8	311.74	6	295.85	7	279.36
13	5	206.04	6	193.27	6	176.45
14	10	091.96 (2)	7	089.20	7	064.72 (2)
15	5	28969.40	6	28944.99	6	28944.25
16	6	838.32	7	819.84 (2)	6	815.01
17	4	698.68	6	682.33	6	677.18
18	3	550.38 (2)	2	534.98	2	529.97
19	2	392.38 (2)	3	378.39	3	373.96 (2)
20	2	225.44	2d	212.41 (2)	3	208.45 (2)
21	1	049.27 (2)	1	037.02	1d	033.72 (2)
22	2	27863.70	1d	27852.29 (2)	2	27849.91 (2)
23	1	668.01	6	657.42 (3)	1	655.93 (2)
24	1	462.66	1	452.29 (3)	1	452.29 (3)
25	0	246.98	1	237.30 (2)	1	237.30 (2)
26	2	020.51	0	013.57		
27	0	26783.35				
28	0d	534.71				
29	3	274.23 (2)				

		P_3		P_2		P_1
4					1	29688.87
5	1	29710.31			1	632.45
6	2	634.08 (2)	10	29606.30 (3)	3	566.77
7	2	550.11	2	525.21	2	492.31
8	10	459.84 (2)	4	437.55	10	409.40 (2)
9	4	362.30	4	342.51	5	318.31 (2)
10	6	257.96	5	240.01	6	219.35
11	3	146.35	2	129.89	10	113.26 (2)
12	5	027.40	6	012.45	6	28992.51
13	6	28900.85 (2)	6	28887.19	5	871.33
14	2	766.87	3	754.33	3	740.39 (2)
15	2	625.08	2	613.68	2	601.30
16	2	476.08	2	464.90	2	454.06
17	2	319.13	3d	308.68	2	298.66 (2)
18	2	154.20	2	143.41	2	135.00
19	1	27985.97 (2)	1	27970.74	1	27963.39
20	1d	786.41 (2)	1d	789.73 (2)	1	783.33
21	1	602.80	1	600.25	4	594.36 (2)
22	0	405.30	2	402.40	1	397.36
23	0	198.56	5	195.25 (2)	1	192.07
24	0	26982.58	0	26979.82	6	26978.80 (2)
25	1	757.25	1	754.84		
26	1d	522.64	1d	520.48		

K	INT.	ν (vac)	INT.	ν (vac)	INT	ν (vac)
		$^RQ_{32}$		$^RQ_{21}$		$^QP_{32}$
3	1	30002.84			3	29917.79
4	0	29991.52	2	29967.37	4	877.24
5	0	971.61	1	950.81	2	831.49
6	0	944.61	2	926.38 (2)	0	779.26
7	1	910.60	5	895.14 (2)	0	719.98
8			1d	854.56	0	653.82
9	1	817.21	1	805.95		
10	1	758.79	1	748.30		
11	1	691.73 (2)	0	682.37		
12			10	606.30 (2)		

		$^QP_{21}$		$^QR_{12}$		$^PQ_{12}$
4			1	29792.54	1	29686.22
5	6	29802.05 (2)	1	758.79	1	629.62
6	1	754.22	1	715.32	1	563.58
7	3d	698.03	5	662.44 (2)	1	489.11
8	2	634.08 (2)	6	603.83 (2)	1	406.08
9	1	562.93	1	534.41	5	314.98 (2)
10	0	482.92	00	456.21	00	215.67
11	00	395.75	00	370.09	3	107.47
12	0	299.05			3d	28990.79
13					1d	867.08

These agreements constitute a rigorous check on the assignments.

IV. CALCULATION OF MOLECULAR CONSTANTS

1. Energy expressions[8]

In a multiplet state the energy is written[9] for case *a*

$$T=T^e+G+A\Lambda\Sigma+B_v[J(J+1)-\Omega^2+\bar{G}^2+S^2_{\text{perp}}]+\varphi_i(\Sigma,J)+D_vJ^2(J+1)^2+F_vJ^3(J+1)^3+\cdots. \quad (1)$$

In case *b*

$$T=T^e+G+B_v[K(K+1)-\Lambda^2+\bar{G}^2]+f_i(K,J-K)+\varphi_i(K,J)+D_vK^2(K+1)^2+F_vK^3(K+1)^3+\cdots. \quad (2)$$

The multiplet splitting in case *a* is given by the term, $A\Lambda\Sigma$, while in case *b* it is given by $f_i(K,J-K)$. $\varphi_i(\Sigma,J)$ and $\varphi_i(K,J)$ are both double valued for any value of J whenever $\Lambda>0$. The two values are distinguished by the subscripts *a* and *b*, as is shown in Fig. 1, the strong *Q* branches are transitions from *a* levels and the strong *P* and *R* branches are from *b* levels. The

[8] Mulliken, Rev. Mod. Phys. **2**, 60 (1932).

[9] It should be noted that F_v is a coefficient in the rotational part of the energy expression and is not to be confused with F, used to express rotational energy as a whole.

TABLE III. *Branches of (0,1) band.*

K	INT.	ν (vac)	INT.	ν (vac)	INT.	ν (vac)	K	INT.	ν (vac)	INT.	ν(vac)	INT.	ν (vac)
		R_3		R_2		R_1			R_3		R_2		R_1
1	0	25082.09 (2)			3	24974.16 (2)	15	0	801.24	0	793.38	1	784.10
2	0	090.53			2	25001.14 (2)	16	3	739.36 (2)	0	732.35	1	723.94
3	0	095.75 (2)	00	25067.38	1	020.83	17	1	670.84	1	664.28	1	657.01
4	00	097.73	0	072.76	2d	033.97	18	1	595.27	2	589.45	1	582.67
5	0	095.75 (2)	0	073.72	1	040.93	19	0d	512.66	0	507.15	0	501.46
6	1	089.49	2	069.81	1	041.82	20	1	423.30	1d	417.41	1d	412.33
7	0d	078.84 (2)	1	061.64	2d	037.05	21	0	324.34	1	320.03	0	315.70
8	1	063.21	1	047.72 (2)	3	026.31 (2)	22	2d	218.18 (2)	1d	214.80	1	210.86
9	1	042.70	1	028.67	2	009.93 (2)	23	0d	104.58	0	101.11	0	097.98
10	1	016.37	1	004.25 (3)	2	24987.64	24			1	23978.85	00	23976.13
11	1	24985.53	3	24974.16 (2)	1	959.40	25			0	847.82	0	846.18
12	1	948.36	2	938.09	2	924.96	26					1	708.03
13	1	905.57	3	895.92 (2)	2	884.37	27					00	561.92
14	1	856.60 (2)	1	847.91	1	837.48							
		Q_3		Q_2		Q_1			Q_3		Q_2		Q_1
1			1	25004.25 (3)	00	24909.53	14	3	487.11	3	470.03	4d	460.42
2	3	25026.31 (2)	0	24978.16 (2)	00	911.92	15	3	410.65	1	394.46	5d	386.09
3	1	004.25 (3)	00	961.24	1	907.34	16	3	328.56	3	313.22	4	305.88
4	0	24978.16 (2)	2	939.56	3	895.92 (2)	17	3	240.59	4d	225.94	3	219.37
5	1	947.87	2	913.75	2	877.65	18	4	146.40	4	132.59	5	126.81
6	2	914.25	2	883.66	2	853.65	19	2	046.12	2	033.03	2	027.95
7	2	877.09	2	849.03	2	823.79	20	2	23939.46	1	23926.92	1d	23922.35
8	2	835.59	2	810.03	2	788.50	21	1	826.24	3	814.04	1	810.23
9	2	789.87	2	766.12	2	747.61	22	1	706.05	1	694.58	2	691.02
10	3	739.36	2	717.38	2	701.30	23	1	578.50	0	567.62	0	564.83
11	2	684.08	2	663.55	3	649.49	24	0	442.10	0	433.37	0	431.07
12	2	623.66	1	604.46	3	592.21	25	0	295.42	00	291.66	0	289.53
13	2	558.09	4	539.97	4	529.17	26			00	142.04	0	140.37
		P_3		P_2		P_1			P_3		P_2		P_1
5	00d	24815.34					14	2	136.87	5	126.81 (2)	3	113.99
6							15	1d	039.67	1	030.58	3	019.11
7	1	691.57 (2)	00	24669.72	1	24637.38	16	1	23937.55	0	23929.22	3d	23919.11
8	0	624.75	0	605.44			17	0	830.56	2d	822.65	3	814.04 (2)
9					0d	512.66 (2)	18	0	718.52	0	711.38	0	703.39
10	1d	479.22	1	464.13	1d	442.90	19	0	600.71	0	594.34	00	587.38
11	1	400.35	0	386.41	1	368.28	20	0d	477.77	00	471.87	0	465.62
12	1	317.07	0	304.78	1	288.50	21	0	348.94			00	338.16
13	4d	229.34	2d	218.18 (2)	3	203.72	22					00	204.87

TABLE IV.

(a) *Branches of (1,1) band (observed).*

K	INT.	ν (vac)	INT.	ν (vac)	INT.	ν (vac)
		Q_3		Q_2		Q_1
4					0	26853.37
5	0	26898.78	0d	26865.48	0	826.68
6	1	854.99	00	825.44	1	792.65
7	1	805.57	1	779.02	2	750.88
8	2	750.88 (2)	0	726.64	1	702.11
9	0	689.55	2d	667.27 (2)	2	646.10
10	1	622.13	0	602.24	1	582.82
11	0d	548.20	1d	530.47 (2)	1d	512.81 (2)
12	1d	467.75	1d	451.57	1	435.07
13	0d	380.59	1d	367.66	1	350.83 (2)
14	3	287.39 (2)				
15	0d	184.90	1	160.78	1	159.50 (2)
16					0	052.90 (2)

(b) *Branches of (1,1) band (calculated by 4 band combinations).*

	Q_3	Q_2	Q_1
4			26852.28
5	26898.83	26865.33	826.71
6	854.62	825.22	792.49
7	805.66	778.87	750.79
8	750.53	725.84	701.94
9	689.69	667.57	645.99
10	622.07	602.20	582.99
11	548.27	530.24	512.57
12	467.70	451.84	435.29
13	380.47	367.65	350.77
14	286.15		
15	184.80	160.33	159.50
16			052.90

difference $\varphi_{ib}(K)-\varphi_{ia}(K)=\Delta\nu_{iba}(K)$ is known as Λ type doubling.

2. Multiplet splitting in the $^3\Sigma$ state

The energy in the lower state is represented by Eq. (2) since a Σ state is strictly case *b*. The term $\varphi_i(K, J)=0$ since $\Lambda=0$. Corresponding to the different values of J, the total angular momentum quantum number, the term $f_i(K, J-K)$ has the following values.[8]

$$J=K+1, \quad f_1=-\epsilon[1-3/(2K+3)]+\gamma K \tag{3}$$

$$J=K, \quad f_2=2\epsilon-\gamma \tag{4}$$

$$J=K-1, \quad f_3=-\epsilon[1+3/(2K-1)]-\gamma(K+1) \tag{5}$$

ϵ and γ being constants. Subtracting (3) from (4) and (5) from (4),

$$\Delta f_{21}(K)=3\epsilon[1-1/(2K+3)]-\gamma(K+1), \tag{6}$$

$$\Delta f_{23}(K)=3\epsilon[1+1/(2K-1)]+\gamma(K). \tag{7}$$

Experimentally $\Delta f_{21}(K)$ and $\Delta f_{23}(K)$ were observed by taking the differences.[5]

TABLE V. $\Delta_2F_i''(K)=R_i(K-1)-P_i(K+1)$.

K	(0,0) band $\Delta_2F_3''(K)$	$\Delta_2F_2''(K)$	$\Delta_2F_1''(K)$	(1,0) band $\Delta_2F_3''(K)$	$\Delta_2F_2''(K)$	$\Delta_2F_1''(K)$	(0,1) band $\Delta_2F_3''(K)$	$\Delta_2F_2''(K)$	$\Delta_2F_1''(K)$
2	163.99								
3	229.77	229.58	229.69			228.92			
4	294.57	294.75	293.66	294.41		293.93	280.41		
5	358.77	358.79	358.14	359.04	357.96	358.27			
6	422.96	422.51	422.41	423.09	422.56	422.36	404.18	404.00	403.55
7	486.41	486.09	485.58	486.39	486.13	485.74	464.74	464.37	
8	549.20	548.82	548.72	549.33	549.01	548.63			524.39
9	611.34	610.95	610.68	611.31	610.96	610.56	583.99	583.59	583.41
10	672.24	672.02	671.73	672.43	672.16	671.77	642.35	642.26	641.65
11	732.46	732.25	732.03	732.50	732.28	731.92	699.80	699.47	699.14
12	791.67	791.37	791.17	791.73	791.43	791.11	756.19	755.98	755.68
13	850.11	849.50	849.34	849.83	849.50	849.39	811.49	811.28	810.97
14	906.83	906.73	906.33	907.03	906.31	906.19	865.90	865.34	865.26
15	962.55	962.30	962.11	962.46	962.18	961.90	919.05	918.69	918.37
16	1016.93	1016.94	1016.45	1016.76	1016.13	1016.32	970.68	970.73	970.06
17	1069.97	1069.77	1069.38	1070.53	1069.82	1069.60	1020.84	1020.97	1020.55
18	1121.52	1121.23	1120.97	1121.50	1121.22	1121.11	1070.13	1069.94	1069.63
19	1171.68	1171.46	1171.10	1171.65	1171.22	1170.84	1117.50	1117.98	1117.05
20	1219.78	1219.69	1219.57	1219.78	1219.59	1219.68	1163.72		1163.30
21	1266.89	1266.62	1266.52	1266.95	1265.97	1266.49			1207.46
22	1312.01	1311.76	1311.46	1311.86	1311.54	1311.02			
23	1355.26	1355.10	1354.91	1355.11	1354.77	1355.79			
24	1396.92	1396.49	1396.60	1396.95	1396.47				
25	1436.43		1435.91	1436.68	1436.44				
26	1476.02		1474.14						
27			1510.35						

TABLE VI. $\Delta_2F_{ib}'(K)=R_i(K)-P_i(K)$.

K	(0,0) band $\Delta_2F_{3b}'(K)$	$\Delta_2F_{2b}'(K)$	$\Delta_2F_{1b}'(K)$	(0,1) band $\Delta_2F_{3b}'(K)$	$\Delta_2F_{2b}'(K)$	$\Delta_2F_{1b}'(K)$	(1,0) band $\Delta_2F_{3b}'(K)$	$\Delta_2F_{2b}'(K)$	$\Delta_2F_{1b}'(K)$
2	111.07	124.26	155.87						
3	167.85	180.10	202.38						
4	224.54	235.07	251.22						236.17
5	280.34	287.67	300.87	280.41			262.89		282.22
6	334.22	339.96	350.09				312.15	317.38	328.37
7	387.27	391.48	399.80	387.27	391.92	399.67	361.52	366.31	374.63
8	438.74	442.16	448.77	438.46	442.28		409.43	413.42	420.51
9	488.60	491.70	497.00			497.27	456.48	459.54	466.72
10	537.58	540.11	544.56	537.65	540.12	544.74	501.94	504.72	505.08
11	585.00	587.15	591.00	585.18	587.75	591.12	546.23	548.73	549.18
12	631.47	633.15	636.50	631.29	633.31	636.46	589.30	591.38	597.27
13	676.11	678.00	680.65	676.23	677.74	680.65	631.26	632.80	636.16
14	719.59	721.05	723.53	719.73	721.10	723.49	671.67	672.75	675.57
15	761.43	763.07	764.91	761.57	762.80	764.99	710.81	711.13	713.68
16	801.63	802.89	804.73	801.81	803.13	804.83	748.65	748.33	750.54
17	840.15	841.19	842.99	840.28	841.63	842.97	788.34	783.28	785.94
18	877.01	878.09	879.47	876.75	878.07	879.28	803.86	817.54	819.17
19	911.68	912.71	914.05	911.95	912.81	914.08	836.61	849.10	850.65
20	944.77	945.57	946.80	945.53	945.54	946.71	885.84	878.64	880.52
21	975.43	976.24	977.48	975.30		977.54	907.62	906.54	908.73
22	1004.34	1005.04	1006.24		1005.16	1005.99	932.39	932.19	937.23
23	1030.95	1031.51	1032.54				955.64	956.06	962.13
24	1054.88	1055.70	1056.25				976.74	977.10	984.59
25	1076.91	1077.14	1078.61					996.51	
26	1096.50		1099.80					1013.75	
27	1115.46								

$$\begin{aligned}\Delta f_{21}(K)&=Q_1(K)-{}^QR_{12}(K)\\&={}^QP_{21}(K)-Q_2(K)\\&=P_1(K)-{}^PQ_{12}(K)\\&={}^RQ_{21}(K)-R_2(K),\end{aligned}\tag{8}$$

$$\begin{aligned}\Delta f_{23}(K)&=Q_3(K)-{}^QP_{32}(K)\\&={}^QR_{23}(K)-Q_2(K)\\&={}^PQ_{23}(K)-P_2(K)\\&=R_3(K)-{}^RQ_{32}(K).\end{aligned}\tag{9}$$

The differences defined in this way are all positive.

The satellites corresponding to $\Delta f_{21}(K)$ are easily picked out by observation while those belonging to $\Delta f_{23}(K)$ are less intense and in very many cases coincide with lines of greater intensity. For this reason, the constants, ϵ and γ, were determined by averaging all observed values of $\Delta f_{21}(K)$, ignoring coincidences, and fitting the resulting points by least squares. The values of ϵ and γ were then used to calculate the values of $\Delta f_{23}(K)$. The satellites corresponding to $\Delta f_{23}(K)$ could then be assigned by using relations (9).

TABLE VII. $\Delta_1F_{iba}'(K+\frac{1}{2})=R_i(K)-Q_i(K)$; $\Delta_1F_{iab}'(K-\frac{1}{2})=Q_i(K)-P_i(K)$.

K	$\Delta_1F_{3ba}'(K+\frac{1}{2})$	$\Delta_1F_{3ab}'(K-\frac{1}{2})$	$\Delta_1F_{2ba}'(K+\frac{1}{2})$	$\Delta_1F_{2ab}'(K-\frac{1}{2})$	$\Delta_1F_{1ba}'(K+\frac{1}{2})$	$\Delta_1F_{1ab}'(K-\frac{1}{2})$	K	$\Delta_1F_{3ba}'(K+\frac{1}{2})$	$\Delta_1F_{3ab}'(K-\frac{1}{2})$	$\Delta_1F_{2ba}'(K+\frac{1}{2})$	$\Delta_1F_{2ab}'(K-\frac{1}{2})$	$\Delta_1F_{1ba}'(K+\frac{1}{2})$	$\Delta_1F_{1ab}'(K-\frac{1}{2})$
			(0,0) band							(0,0) band			
1	32.25						15	390.44	370.99	399.03	364.04	397.82	367.09
2	62.27	48.80	78.43	45.83	89.45		16	410.68	390.95	418.90	383.99	417.93	386.80
3	91.36	76.49	106.28	73.82	113.43	88.95	17	430.11	410.04	438.17	403.02	437.40	405.59
4	119.68	104.86	133.53	101.54	138.00	113.22	18	448.65	428.36	456.73	421.36	455.90	423.57
5	147.73	132.61	159.84	127.83	163.31	137.56	19	466.13	445.55	474.11	438.60	473.41	440.64
6	175.06	159.26	186.35	153.61	187.96	162.13	20	482.72	462.05	490.49	455.08	489.98	456.82
7	201.73	185.54	212.23	179.25	213.27	186.53	21	498.17	477.26	505.92	470.32	505.41	471.96
8	227.83	210.91	237.57	204.59	237.94	210.83	22	513.18	491.16	520.29	484.75	519.93	486.31
9	252.93	235.67	262.63	229.07	262.34	234.66	23	526.13	504.82	533.50	498.01	533.31	499.23
10	277.61	259.97	286.83	253.28	286.53	258.03	24	537.67	517.21	545.30	510.40	544.74	511.51
11	301.44	283.56	310.49	276.66	309.81	281.19	25	548.42	528.49	555.82	521.32	556.11	522.50
12	325.06	306.41	333.62	299.53	332.87	303.63	26	558.27	538.23	564.28	531.91	567.32	532.48
13	347.43	328.68	356.22	321.78	355.23	325.42	27	566.80	548.68				540.88
14	369.32	350.27	377.77	343.28	376.95	346.58	28	573.55					
			(0,1) band							(0,1) band			
2					89.22		15	390.59	370.98	398.92	363.88	398.01	366.98
3	91.50		106.14		113.49		16	410.80	391.01	419.13	384.00	418.06	386.77
4	119.57		133.16		138.05		17	430.25	410.03	438.34	403.29	437.64	405.33
5	147.88	132.53	159.97		163.28		18	448.87	427.88	456.86	421.21	455.86	423.42
6	175.24		186.15		188.17		19	466.54	445.51	474.12	438.69	473.51	440.57
7	201.75	185.50	212.61	179.31	213.26	186.41	20	483.84	461.69	490.49	455.05	489.98	456.73
8	227.62	210.84	237.69	204.59	237.81		21	498.00	477.30	505.99		505.47	472.07
9	252.83		262.55		262.32	234.95	22	512.13	490.40	520.22		519.84	486.15
10	277.51	260.14	286.87	253.25	286.34	258.40	23	526.08		533.49		533.15	
11	301.45	283.73	310.61	277.14	309.91	281.21	24			545.48		545.06	
12	324.70	306.59	333.63	299.68	332.75	303.71	25			556.16		556.65	
13	347.48	328.75	355.95	321.79	355.20	325.45	26					567.66	
14	369.49	350.24	377.88	343.22	377.06	346.43							
			(1,0) band							(1,0) band			
2					82.72		15	346.58	325.09	379.82	331.31	370.73	342.95
3					107.01		16	366.49	344.32	393.39	354.94	389.59	360.95
4	84.70		123.10		129.79	106.38	17	386.41	362.24	409.63	373.65	407.42	378.52
5	113.70		147.83		153.26	128.96	18	408.79	379.55	425.97	391.57	424.20	394.97
6	139.79	123.10	172.58	144.80	176.65	151.72	19	407.68	396.18	441.45	407.65	440.08	410.57
7	165.64	146.51	196.74	169.57	200.16	174.47	20	430.20	406.41	455.96	422.68	455.40	425.12
8	190.30	171.22	220.77	192.65	223.61	196.90	21	446.81	439.03	469.77	436.77	469.37	439.36
9	214.55	194.88	243.18	216.36	247.66	219.06	22	461.15	446.47	482.30	449.89	484.68	452.55
10	238.00	218.48	265.55	239.17	264.59	240.49	23	473.99	458.40	493.89	462.17		463.86
11	260.95	240.99	287.24	261.49	288.57	260.61	24	486.19	469.45	504.63	472.47		473.49
12	283.18	263.05	307.98	283.40	310.42	286.85	25	496.66	480.08	514.05	482.46		
13	304.96	284.34	326.72	306.08	331.04	305.12	26		489.73	520.66	493.09		
14	326.07	305.19	337.88	334.87	351.24	324.33	27		497.87				

In Fig. 2 are plotted the average observed values of $\Delta f_{21}(K)$ and $\Delta f_{23}(K)$ (including coincidences) against K. The curves represent Eqs. (6) and (7) with the following values of the constants:

$$3\epsilon=2.29\ \text{cm}^{-1},\quad \gamma=-0.132\ \text{cm}^{-1}.$$

The approximate agreement of the full circles in Fig. 2 with the curve establishes the adequacy of Eqs. (6) and (7) in this case.

3. Fine structure of the $^3\Pi$ state

a. Λ type doubling. The Λ type doubling, as deducible from measured frequencies, is really the average of two successive doublings, i.e.,

$$2\Delta\nu_{iba}(K+\tfrac{1}{2})=\Delta_1F_{iba}'(K+\tfrac{1}{2})-\Delta_1F_{iab}'(K+\tfrac{1}{2})$$
$$=\Delta\nu_{iba}(K)+\Delta\nu_{iba}(K+1),$$

where

$$\Delta_1F_{iba}'(K+\tfrac{1}{2})=R_i(K)-Q_i(K),$$
$$\Delta_1F_{iab}'(K-\tfrac{1}{2})=Q_i(K)-P_i(K);$$

$\Delta\nu_{iba}(K+\frac{1}{2})$ plotted against K is shown in Fig. 3.

These values of the Λ type doubling can be used, as was done in the case of the first positive nitrogen bands by Naudé,[5] to determine whether the $^3\Pi$ level is normal or inverted. According to theory[10] the Λ type doubling in case *a* should behave as follows: The $^3\Pi_0$ level should show a comparatively large doubling independent of J, which should therefore exist even for $J=0$. The doubling of the $^3\Pi_1$ levels should be proportional to $J(J+1)$ and that of the $^3\Pi_2$ levels should be very small and approximately proportional to $J^2(J+1)^2$. In case *b* all three levels should show doublings approximately propor-

[10] Hill and Van Vleck, Phys. Rev. **32**, 250 (1928); J. H. Van Vleck, Phys. Rev. **33**, 467 (1929); R. S. Mulliken, Rev. Mod. Phys. **3**, 145 (1931).

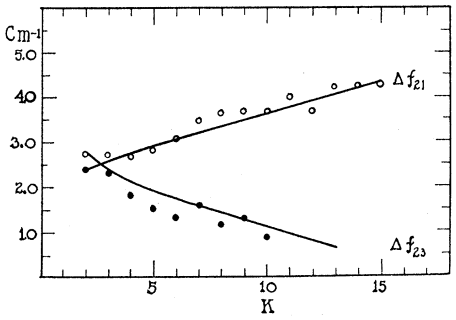

FIG. 2. Multiplet splitting in the $^3\Sigma$ state. Circles represent average of all observed values of $\Delta f_{21}(K)$. Dots represent average of all observed values of $\Delta f_{23}(K)$. Curves are drawn through points calculated, using $3\epsilon = 2.29$ cm^{-1}, $\gamma = -0.132$ cm^{-1}.

tional to $K(K+1)$. The curves in Fig. 3 do not correspond to either of these cases but are qualitatively in consonance with the assumption that the $^3\Pi$ state is intermediate between cases *a* and *b*, and that the high frequency set of levels, $^3\Pi_{high}$ is $^3\Pi_0$ that $^3\Pi_{med}$ is $^3\Pi_1$ and $^3\Pi_{low}$ is $^3\Pi_2$, that is, the $^3\Pi$ level is inverted. The method of distinguishing between these sub-levels by means of "missing lines" is not applicable here because of the large number of lines in the neighborhood of the origins.

The erratic behavior of the Λ type doubling in the $v'=1$ state is due to the perturbations in that state. The assignments, however, are checked by $\Delta_2 F''$ combinations.

b. Multiplet splitting. In the absence of a closed energy expression for the case of coupling intermediate between cases *a* and *b*, it seems that one can at best obtain a rough value of the coefficient, A, by assuming that case *a* is approximated at the lowest values of J. Then:

$$^3\Pi_2(2) - {}^3\Pi_1(1) = {}^3\Pi_1(1) - {}^3\Pi_0(0) = A + B$$

where J is the argument[4] or

$$^3\Pi_2(1) - {}^3\Pi_1(1) = {}^3\Pi_1(1) - {}^3\Pi_0(1) = A + B$$

where K is the argument. Λ type doubling is too great to neglect but a fair value should be obtained by averaging the *a* and *b* separations. These separations are observed by using

$$^3\Pi_{1a}(K) - {}^3\Pi_{0a}(K) = {}^QP_{32}(K) - Q_2(K),$$

$$^3\Pi_{2a}(K) - {}^3\Pi_{1a}(K) = {}^QR_{12}(K) - Q_2(K),$$

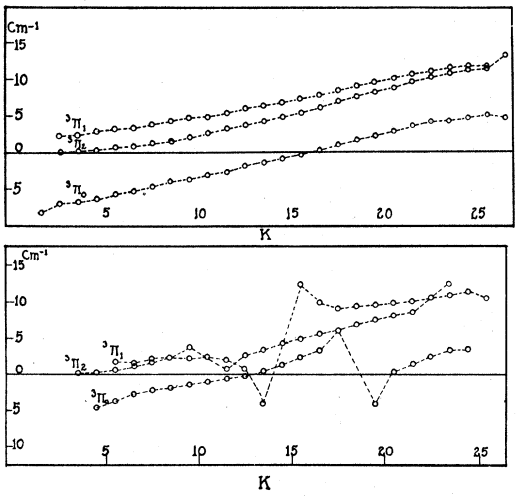

FIG. 3. Λ type doubling in the $v'=0$ and $v'=1$ levels of the $^3\Pi$ state. $\Delta\nu_{iba}$ $(K+1/2)$ plotted against $(K+1/2)$. Upper figure is for $v=0$. Lower figure is for $v=1$. Dotted lines are drawn between points corresponding to the same component of the $^3\Pi$ state. Erratic behavior of Λ type doubling when $v=1$ is due to perturbations.

$$^3\Pi_{1b}(K) - {}^3\Pi_{0b}(K) = {}^PQ_{23}(K+1) - P_3(K+1),$$

$$^3\Pi_{2b}(K) - {}^3\Pi_{1b}(K) = {}^PQ_{12}(K+1) - P_2(K+1).$$

These were plotted near the origin and extrapolated to $K=1$, when necessary. The values of A so determined are

$$^3\Pi_1 - {}^3\Pi_0, \quad A = -66 \text{ cm}^{-1},$$

$$^3\Pi_2 - {}^3\Pi_1, \quad A = -97 \text{ cm}^{-1}.$$

This considerable disagreement is probably due to the fact that the pure case *a* energy expression is inadequate even for these low values of J. Similar but smaller differences have been found in PH[4] and in the first positive bands of nitrogen.[5]

4. Rotational and vibrational constants

The constants B_v, D_v and F_v are evaluated by taking the second differences,

$$\Delta_2 F_i(K) = F_i(K+1) - F_i(K-1). \qquad (10)$$

Eqs. (3), (4) and (5) show that in a $^3\Sigma$ state, the best value of the constants should be obtained by taking second differences of F_2 since the term $f_i(K, J-K)$ is constant for this component of the multiplet. Now

TABLE VIII. Λ *type doubling.*

	(0,0) band			(0,1) band			(1,0) band		
$(K+\frac{1}{2})$	$\Delta\nu_{3ba}(K+\frac{1}{2})$	$\Delta\nu_{2ba}(K+\frac{1}{2})$	$\Delta\nu_{1ba}(K+\frac{1}{2})$	$\Delta\nu_{3ba}(K+\frac{1}{2})$	$\Delta\nu_{2ba}(K+\frac{1}{2})$	$\Delta\nu_{1ba}(K+\frac{1}{2})$	$\Delta\nu_{3ba}(K+\frac{1}{2})$	$\Delta\nu_{2ba}(K+\frac{1}{2})$	$\Delta\nu_{1ba}(K+\frac{1}{2})$
1.5	−8.22								
2.5	−7.11	2.30	0.25						
3.5	−6.75	2.37	.10						0.31
4.5	−6.46	2.85	.22	−6.48			−4.70		.41
5.5	−5.76	3.11	.59				−3.36	1.51	.77
6.5	−5.24	3.55	.71	−5.13	3.42	0.83	−2.79	1.50	1.09
7.5	−4.59	3.82	1.22	−4.54	4.01		−2.29	2.04	1.63
8.5	−3.92	4.25	1.64			1.43	−1.96	2.20	2.27
9.5	−3.52	4.67	2.15	−3.65	4.65	1.96	−1.49	2.00	3.58
10.5	−2.97	5.08	2.67	−3.11	4.86	2.56	−1.05	2.03	
11.5	−2.48	5.48	3.09	−2.57	5.46	3.10	− .58	1.92	.86
12.5	−1.81	5.92	3.72	−2.02	5.92	3.65	− .11	.95	2.65
13.5	−1.42	6.47	4.32	−1.38	6.36	4.38	.49	−4.07	3.35
14.5	− .83	6.86	4.94	− .74	7.00	5.04	1.13		4.14
15.5	− .25	7.52	5.51	− .21	7.46	5.62	2.12	12.44	4.89
16.5	.32	7.94	6.17	.38	7.92	6.36	3.43	9.87	5.53
17.5	.87	8.40	6.91	1.18	8.56	7.11	6.30	9.03	6.22
18.5	1.55	9.06	7.63	1.73	9.08	7.64		9.16	6.81
19.5	2.04	9.51	8.29	2.42	9.53	8.39	−4.41	9.38	7.48
20.5	2.73	10.08	9.01	3.02		8.95	.17	9.59	8.02
21.5	3.50	10.58	9.55	3.80		9.66	1.37	9.94	8.41
22.5	4.18	11.14	10.35				2.27	10.06	10.41
23.5	4.46	11.55	10.90				3.05	10.71	12.39
24.5	4.59	11.99	11.12				3.49	11.33	
25.5	5.09	11.95	11.81					10.38	
26.5	4.80		13.22						

$$\Delta_2F_2''(K)=4B_v''(K+\tfrac{1}{2})+8D_v''(K+\tfrac{1}{2})^3+12F_v(K+\tfrac{1}{2})^5+\cdots, \quad (11)$$

where terms small in comparison to $12F_v(K+\frac{1}{2})^5$ are dropped. Also

$$\Delta_2F_2''(K)=R_2(K-1)-P_2(K+1). \quad (12)$$

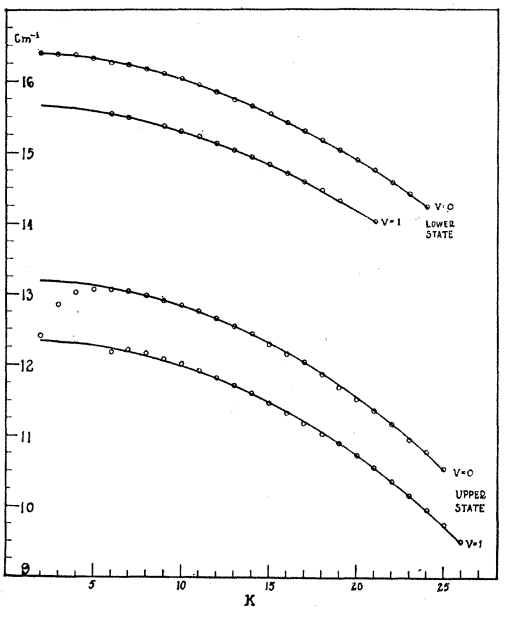

FIG. 4. Observed values of $\Delta_2F_2''(K)/4(K+1/2)$ are represented by circles. Curves are drawn through values calculated by using Table XI. In the case of the upper state observed values of Δ_2F_2' are the average of Δ_2F_{2a} and Δ_2F_{2b}.

The calculation is greatly simplified by dividing $\Delta_2F_2''(K)$ by $4(K+\frac{1}{2})$ giving $B_v''+2D_v''(K+\frac{1}{2})^2+3F_v''(K+\frac{1}{2})^4$. The value of F_v'' was determined by using 3 values of $\Delta_2F_2''/4(K+\frac{1}{2})$ and solving the resulting simultaneous equations. The values of $3F_v''(K+\frac{1}{2})^4$ were then subtracted from the observed values and B_v'' and D_v'' were calculated by least squares.

In the $^3\Pi$ state there should be an expression for Δ_2F_2' similar to Eq. (11) except for Λ type doubling. The theory of Λ type doubling for cases intermediate between *a* and *b* does not permit an exact correction for this, but fairly accurate results should be obtained by using the average,

$$\Delta_2\bar{F}_2'(K)=(\Delta_2F_{2a}'+\Delta_2F_{2b}')/2 \quad \text{where}$$

$$\Delta_2F_{2b}'(K)=R_2(K)-P_2(K), \quad (13)$$

$$\Delta_2F_{2a}'(K)=Q_2(K-1)-Q_2(K+1)-\Delta_2F_2''(K). \quad (14)$$

This procedure was followed in the $^3\Pi_2$ state $(v=0)$ with observations from the (0,0) band, but it cannot be used in the $^3\Pi_2$ state $(v=1)$ because of the perturbation in the Q_2 branch of the (1,0) band (see Figs. 3 and 5). Since taking this average simply amounts to adding the difference of two Λ type doublings to Δ_2F_{2b}', it is sufficiently accurate to add the same term as was added for $v=0$. The correction is small, averaging less than 1 cm^{-1}. In Fig. 4 the circles

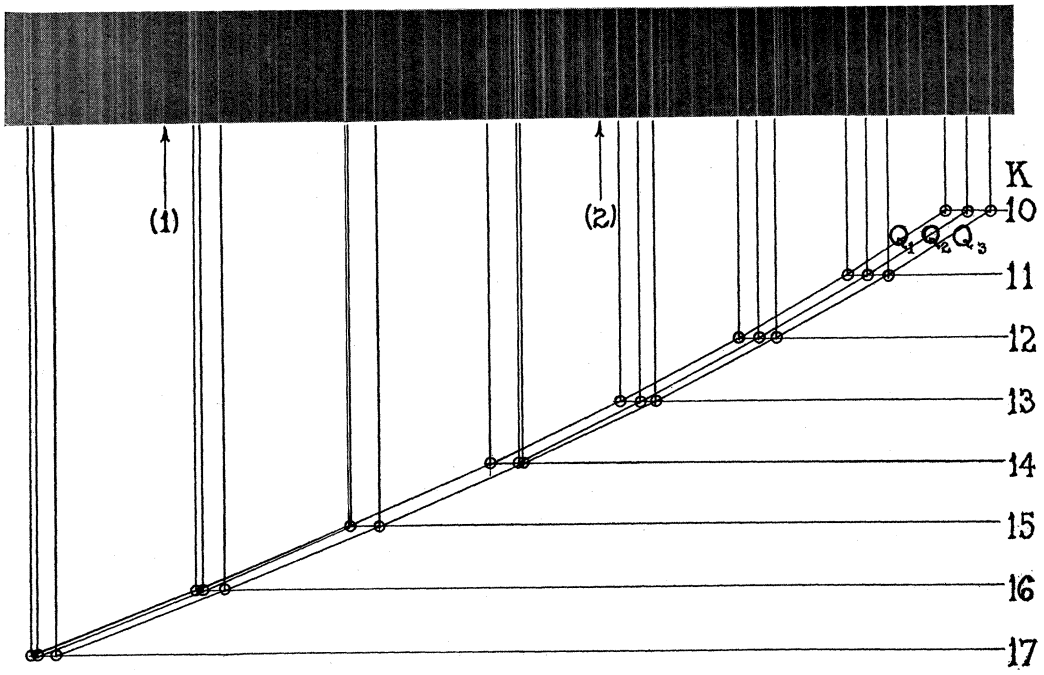

FIG. 5. The perturbation in the Q_2 branch of the (1,0) band. Circles show K plotted against plate position for all three Q branches. Heads of the OH bands at 3484A and 3428A are indicated by arrows; the former being marked (1), the latter (2).

show resulting values divided by $4(K+\frac{1}{2})$ and plotted against K. The Hill and Van Vleck[11] theory of multiplet separation would lead one to expect this curve to be almost constant near the origin and to have an intercept $=B_0'$, while the actual curve bends downward for values of $K<5$. This might be due to an error in assignment, but such an explanation seems improbable due to the fact that combination relations check well near the origin and that intensities of lines assigned to all branches run quite smoothly. Also Δ_2F_{2a}' and Δ_2F_{2b}' differ by less than 1 cm^{-1} near the origin which would hardly be expected if there were an error in assignment, and the $\Delta_2F_2''(K)$ values which are obtained from the same lines fit the theory very well.

Values of $\Delta_2\bar{F}_2'(K)$ for $K<5$ were ignored in computing constants. The calculation was carried out in the same manner as for the $^3\Sigma$ state.

The values of all constants are given in Table XI. In Table IX(a) are tabulated observed values of $[\Delta_2F_2''(K)]/[4(K+\frac{1}{2})]$ and values calculated from the constants. Table IX(b) gives corresponding values for the $^3\Pi$ state. These data are plotted in Fig. 4 with the curves drawn through points calculated from the constants. The differences $\Delta_2F_2(K)$(obs.) $-\Delta_2F_2(K)$(calc.) are also given in Table IX.

B_v and D_v depend upon the vibrational quantum number in the following manner:

$$B_v=B_e-\alpha_e(v+\tfrac{1}{2})+\cdots, \tag{15}$$

$$D_v=D_e+\beta_e(v+\tfrac{1}{2})+\cdots, \tag{16}$$

so that

$$\alpha_e=B_0-B_1, \tag{17}$$

$$\beta_e=D_1-D_0. \tag{18}$$

Using Table I with Eqs. (15)–(18) gives for the lower state,

$$\alpha_e''=0.732\ cm^{-1}$$

$$\beta_e''=-0.053\times10^{-3}\ cm^{-1}$$

$$B_e''=16.793\ cm^{-1}$$

$$D_e''=-1.957\times10^{-3}\ cm^{-1}$$

for the upper state,

$$\alpha_e'=0.841\ cm^{-1},\quad B_e'=13.642\ cm^{-1},$$

$$\beta_e'=\text{very small},\quad D_e'=D_e'=-1.782\ cm^{-1}.$$

[11] Hill and Van Vleck, Phys. Rev. 32, 250 (1928).

TABLE IX (a). $\frac{\Delta_2F_2''(K)}{4(K+\frac{1}{2})}$.

$v=0$				$v=1$			
K	$\frac{\Delta_2F_2''(K)}{4(K+\frac{1}{2})}$ (obs.)	$\frac{\Delta_2F_2''(K)}{4(K+\frac{1}{2})}$ (calc.)	$\Delta_2F_2''(K)$ (obs.) $-\Delta_2F_2''(K)$ (calc.)	K	$\frac{\Delta_2F_2''(K)}{4(K+\frac{1}{2})}$ (obs.)	$\frac{\Delta_2F_2''(K)}{4(K+\frac{1}{2})}$ (calc.)	$\Delta_2F_2''(K)$ (obs.) $-\Delta_2F_2''(K)$ (calc.)
2	16.388	16.403	−0.15	2		15.672	
3	.399	.380	.27	3		.649	
4	.375	.349	.47	4		.619	
5	.309	.310	−.02	5		.581	
6	.250	.265	−.39	6	15.538	.537	0.03
7	.203	.211	−.24	7	.479	.482	−.09
8	.142	.150	−.27	8		.426	
9	.078	.081	−.11	9	.358	15.359	−.04
10	.000	.006	−.25	10	.292	.286	.25
11	15.918	15.923	−.23	11	.206	.205	.05
12	.827	.834	−.35	12	.120	.118	.10
13	.731	.736	−.27	13	.024	.024	.00
14	.633	.632	.06	14	14.920	14.924	−.23
15	.521	.522	−.06	15	.818	.817	.06
16	.408	.405	.20	16	.708	.703	.33
17	.282	.281	.07	17	.585	.585	.00
18	.150	.151	−.07	18	.459	.460	−.07
19	.017	.015	.16	19	.333	.328	.39
20	14.874	14.873	.08	20		.192	
21	.728	.726	.17	21	.044	.049	−.43
22	.575	.572	.27				
23	.416	.414	.19				
24	.250	.250	.00				

TABLE IX (b). $\frac{\Delta_2\bar{F}_2'(K)}{4(K+\frac{1}{2})} = \frac{\Delta_2F_{2a}'(K)+\Delta_2F_{2b}'(K)}{8(K+\frac{1}{2})}$.

$v=0$				$v=1$			
K	$\frac{\Delta_2\bar{F}_2'(K)}{4(K+\frac{1}{2})}$ (obs.)	$\frac{\Delta_2\bar{F}_2'(K)}{4(K+\frac{1}{2})}$ (calc.)	$\Delta_2\bar{F}_2'(K)$ (obs.) $-\Delta_2\bar{F}_2'(K)$ (calc.)	K	$\frac{\Delta_2\bar{F}_2'(K)}{4(K+\frac{1}{2})}$ (obs.)	$\frac{\Delta_2\bar{F}_2'(K)}{4(K+\frac{1}{2})}$ (calc.)	$\Delta_2\bar{F}_2'(K)$ (obs.) $-\Delta_2\bar{F}_2'(K)$ (calc.)
2	12.426	13.200	−7.74	2		12.359	
3	.859	.178	−4.46	3		.337	
4	13.033	.150	−2.11	4		.308	
5	.064	.113	−1.08	5		.272	
6	.059	.070	−.31	6	12.190	.228	−0.99
7	.040	.018	−.42	7	.201	.177	.66
8	12.992	12.960	.96	8	.147	.117	.88
9	.929	.893	1.36	9	.083	.051	.99
10	.850	.817	1.38	10	.007	11.976	1.30
11	.755	.734	.97	11	11.901	.893	.38
12	.654	.642	.60	12	.819	.801	.90
13	.545	.540	.22	13	.708	.702	.32
14	.425	.430	−.24	14	.592	.593	−.06
15	.297	.309	−.74	15	.459	.475	−.99
16	.158	.181	−1.45	16	.332	.348	−1.05
17	.010	.040	−2.10	17	.183	.212	−2.03
18	11.856	11.890	−2.52	18	.038	.065	−2.00
19	.694	.728	−2.57	19	10.879	10.908	−2.34
20	.524	.554	−2.46	20	.708	.741	−2.60
21	.345	.369	−1.98	21	.535	.563	−2.41
22	.161	.171	−.90	22	.352	.374	−1.97
23	10.968	10.961	.75	23	.166	.173	−.66
24	.767	.736	3.13	24	9.966	9.960	.48
25	.555	.498	5.92	25	.765	.735	3.04
				26	.559	.496	6.68

The following relation also exists between constants.

$$\omega_e^2 = -4B_e^3/D_e. \tag{19}$$

This gives the values

$$\omega_e'' = 3111 \text{ cm}^{-1}, \quad \omega_e' = 2387 \text{ cm}^{-1}.$$

By extrapolating the Q_2 branches to the origins, and subtracting, approximate values of $\omega_{\frac{1}{2}}$ may be obtained where $\omega_{\frac{1}{2}} = \omega_e - 2x_e\omega_e$. These values are,

$$\omega_{\frac{1}{2}}'' = 2955 \text{ cm}^{-1}, \quad \omega_{\frac{1}{2}}' = 1986 \text{ cm}^{-1}.$$

By comparison of the values of ω_e obtained from Eq. (19) with those of $\omega_{\frac{1}{2}}$ it can be deduced that $x_e''\omega_e'' = 73$ cm^{-1} and $x_e'\omega_e' = 200$ cm^{-1}, but it is doubtful whether the constants in Eq. (19) are known with sufficient accuracy to justify much confidence in these values of $x_e\omega_e$. Certainly estimates of the energies of dissociation based upon them would be highly precarious.

F_v is a function of v, but it is not worth while

TABLE X. *Multiplet splitting in the lower state.*

K	$\Delta f_{21}(K)$ (obs.) (average)	$\Delta f_{21}(K)$ (calc.)	$\Delta f_{23}(K)$ (obs.) (average)	$\Delta f_{23}(K)$ (calc.)
2	2.72	2.36	2.40	2.80
3	2.71	2.57	2.30	2.36
4	2.67	2.74	1.81	2.10
5	2.80	2.90	1.52	1.89
6	3.06	3.06	1.30	1.71
7	3.46	3.21	1.60	1.55
8	3.66	3.36	1.16	1.40
9	3.66	3.50	1.29	1.25
10	3.67	3.64	.85	1.10
11	4.00	3.78		
12	3.70	3.92		
13	4.22	4.06		
14	4.25	4.19		
15	4.27	4.33		

TABLE XI. *Molecular constants.*

	$^3\Sigma$ STATE	$^3\Pi$ STATE
$v=0$	$B_0''=16.427$ cm^{-1}	$B_0'=13.222$ cm^{-1}
	$D_0''=-1.931\times10^{-3}$ cm^{-1}	$D_0'=-1.782\times10^{-3}$ cm^{-1}
	$F_0''=1.31\times10^{-7}$ cm^{-1}	$F_0'=-3.21\times10^{-7}$ cm^{-1}
$v=1$	$B_1''=15.695$ cm^{-1}	$B_1'=12.381$ cm^{-1}
	$D_1''=-1.878\times10^{-3}$ cm^{-1}	$D_1'=-1.798\times10^{-3}$ cm^{-1}
	$F_1''=1.41\times10^{-7}$ cm^{-1}	$F_1'=-2.42\times10^{-7}$ cm^{-1}
	$B_e''=16.793$ cm^{-1}	$B_e'=13.642$ cm^{-1}
	$D_e''=-1.957\times10^{-3}$ cm^{-1}	$D_e'\cong D_0'=-1.782\times10^{-3}$ cm^{-1}
	$\alpha_e''=0.732$ cm^{-1}	$\alpha_e'=0.841$ cm^{-1}
	$\beta_e''=-0.053\times10^{-3}$ cm^{-1}	β_e' very small
	$I_e''=1.647\times10^{-40}$ g cm^2	$I_e'=2.028\times10^{-40}$ g cm^2
	$r_e''=1.027\times10^{-8}$ cm	$r_e'=1.139\times10^{-8}$ cm

to distinguish between F_e and F_v. F_e may be calculated by using

$$F_e=(D_e^2/B_e)[2-\alpha_e\omega_e/6B_e^2], \qquad (20)$$

giving

$$F_e''=1.51\times10^{-7}, \quad F_e'=0.468\times10^{-7}$$

as compared with

$$F_0''=1.31\times10^{-7}, \quad F_0'=-3.21\times10^{-7},$$

$$F_1''=1.41\times10^{-7}, \quad F_1'=-2.42\times10^{-7}.$$

The agreement of F_e'' with F_0'' and F_1'' is as good as can be expected. F_e' does not agree with the values of F_0' and F_1', being of opposite sign. This is probably partly due to the fact that the constants used in calculating F_e' are not so reliable as those used in calculating F_e'' and partly to the fact that the values of F_0' and F_1' are erroneous because the observed values of $\Delta_2F_2'/4(K+\frac{1}{2})$ do not fit the assumed formula (see Fig. 4).

The constants, I_e and r_e, were calculated from B_e in the usual manner (see Table XI).

JANUARY 1, 1936 PHYSICAL REVIEW VOLUME 49

The Excitation of the Auroral Green Line by Metastable Nitrogen Molecules

JOSEPH KAPLAN, *University of California at Los Angeles*

(Received September 13, 1935)

The excitation of the auroral green line in tubes which show the two new afterglow spectra of nitrogen is described. The conditions of excitation in the present experiments are compared with those in the night-sky and in the aurora borealis. It is proposed that in both of these phenomena the $^1S_0$ state of oxygen which is responsible for the green line is produced by collisions between oxygen atoms and metastable nitrogen molecules in the $A^3\Sigma$ state. Processes by which oxygen atoms may be excited to the $^1S_0$ state in the night-sky and in auroras which have been proposed by other authors are discussed.

I. INTRODUCTION

ONE of the most striking characteristics of the auroral green line in both auroral and night-sky spectra is that, with the exception of the two relatively weak red lines λ6300 and λ6363, it is the only oxygen line present. This peculiar fact immediately suggests of course that some special process or processes are responsible for the production of this line. Naturally, many such processes have been proposed during the few years since the definite identification of this line as the transition $^1S_0\rightarrow{}^1D_2$ in oxygen. Some of these proposals will be discussed briefly later in the paper. My own feeling has been that the most conclusive way by which to explain the excitation of the green line is to produce it in a laboratory experiment in such a way that both its appearance and mode of production fit in with observed and hypothetical facts about the upper atmosphere.

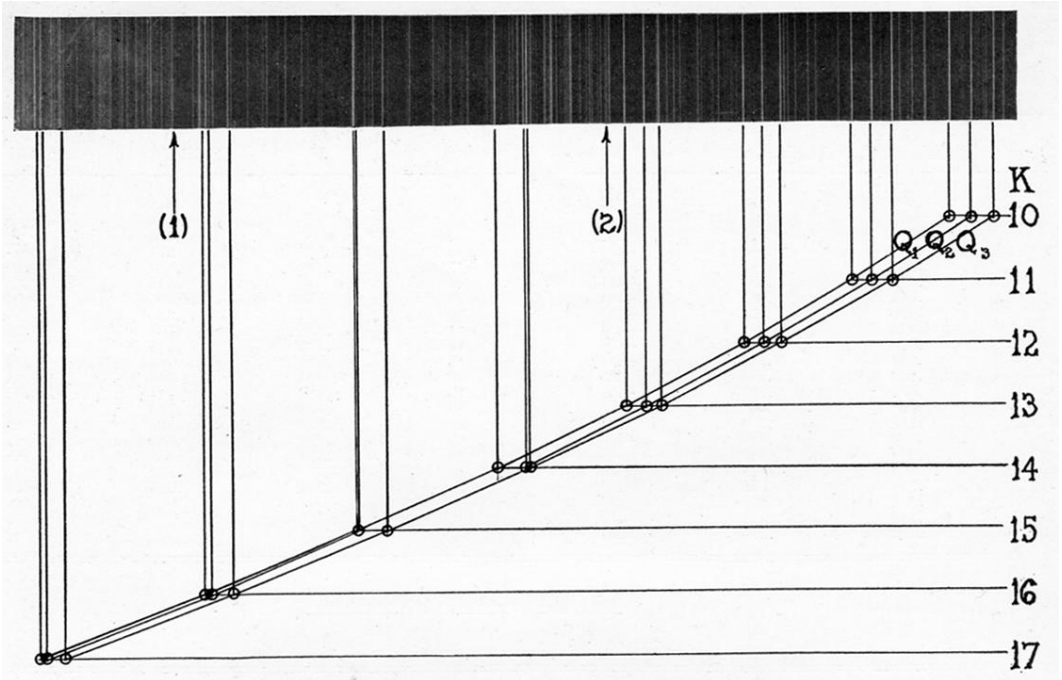

FIG. 5. The perturbation in the Q_2 branch of the (1,0) band. Circles show K plotted against plate position for all three Q branches. Heads of the OH bands at 3484A and 3428A are indicated by arrows; the former being marked (1), the latter (2).